AD-A130 277 RESONANCE FLUORESCENCE OF A TWO-LEVEL ATOM NEAR A METAL 1/1
SURFACE(U) ROCHESTER UNIV NY DEPT OF CHEMISTRY
X HUANG ET AL. JUN 83 UROCHESTER/DC/83/TR-36
UNCLASSIFIED N00014-80-C-0472 F/G 7/4 NL

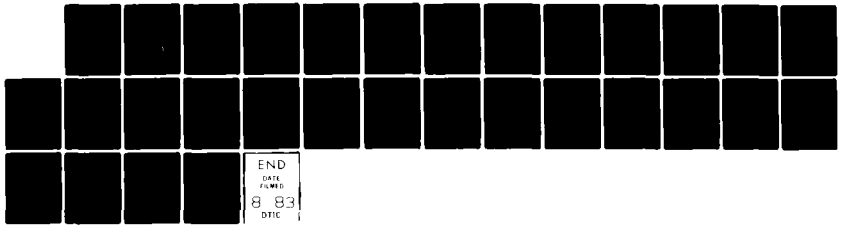

END
DATE FILMED
8 83
DTIC

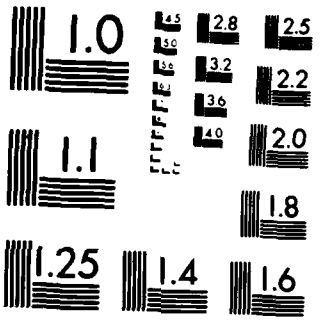

(12)

OFFICE OF NAVAL RESEARCH

Contract N00014-80-C-0472

Task No. NR 056-749

TECHNICAL REPORT No. 36

Resonance Fluorescence of a Two-Level Atom Near a Metal Surface

by

Xi-Yi Huang, Jui-teng Lin and Thomas F. George

Prepared for Publication

in

Journal of Chemical Physics

Department of Chemistry
University of Rochester
Rochester, New York 14627

June 1983

Unclassified

SECURITY CLASSIFICATION OF THIS PAGE (When Data Entered)

REPORT DOCUMENTATION PAGE		READ INSTRUCTIONS BEFORE COMPLETING FORM
1. REPORT NUMBER UROCHESTER/DC/83/TR-36	2. GOVT ACCESSION NO. A130277	3. RECIPIENT'S CATALOG NUMBER
4. TITLE (and Subtitle) Resonance Fluorescence of a Two-Level Atom Near a Metal Surface		5. TYPE OF REPORT & PERIOD COVERED 6. PERFORMING ORG. REPORT NUMBER
7. AUTHOR(s) Xi-Yi Huang, Jui-teng Lin and Thomas F. George		8. CONTRACT OR GRANT NUMBER(s) N00014-80-C-0472
9. PERFORMING ORGANIZATION NAME AND ADDRESS Department of Chemistry University of Rochester Rochester, New York 14627		10. PROGRAM ELEMENT, PROJECT, TASK AREA & WORK UNIT NUMBERS NR 056-749
11. CONTROLLING OFFICE NAME AND ADDRESS Office of Naval Research Chemistry Program Code 472 Arlington, Virginia 22217		12. REPORT DATE June 1983 13. NUMBER OF PAGES 25
14. MONITORING AGENCY NAME & ADDRESS(if different from Controlling Office)		15. SECURITY CLASS. (of this report) 15a. DECLASSIFICATION/DOWNGRADING SCHEDULE

16. DISTRIBUTION STATEMENT (of this Report)

This document has been approved for public release and sale; its distribution is unlimited.

17. DISTRIBUTION STATEMENT (of the abstract entered in Block 20, if different from Report)

18. SUPPLEMENTARY NOTES

Prepared for publication in the Journal of Chemical Physics

19. KEY WORDS (Continue on reverse side if necessary and identify by block number)

RESONANCE FLUORESCENCE	POWER SPECTRUM
TWO-LEVEL ATOM	SURFACE-DRESSED BLOCH EQUATIONS
METAL SURFACE	LASER BANDWIDTH
REFLECTED FIELD	PHASE-DIFFUSION MODEL
POPULATION INVERSION	OSCILLATORY BEHAVIOR

20. ABSTRACT (Continue on reverse side if necessary and identify by block number) A derivation of surface-dressed optical Bloch equations, involving a treatment of surface-reflected photons and a surface plasmon resonance, is presented for a collision-damped two-level atom near or adsorbed on a metal surface. Effects of the laser bandwith are included by means of a phase-diffusion model for the driving field. In the weak-field or large detuning limit, the population inversion and resonance fluorescence spectrum are obtained analytically. These quantities along with the surface-induced phase-decay constant of the adatom show strong oscillatory behavior as a function of the adatom-surface distance.

DD FORM 1 JAN 73 1473 EDITION OF 1 NOV 65 IS OBSOLETE
S/N 0102-LF-014-6601

Unclassified

SECURITY CLASSIFICATION OF THIS PAGE (When Data Entered)

Journal of Chemical Physics, in press

RESONANCE FLUORESCENCE OF A TWO-LEVEL ATOM NEAR A METAL SURFACE

Xi-Yi Huang,[a]* Jui-teng Lin[b] and Thomas F. George[a]

[a]Department of Chemistry, University of Rochester
Rochester, New York 14627

[b]Laser Physics Branch, Optical Sciences Division, Naval Research Laboratory
Washington, D.C. 20375

Abstract

A derivation of surface-dressed optical Bloch equations, involving a treatment of surface-reflected photons and a surface plasmon resonance, is presented for a collision-damped two-level atom near or adsorbed on a metal surface. Effects of the laser bandwidth are included by means of a phase-diffusion model for the driving field. In the weak-field or large detuning limit, the poplulation inversion and resonance fluorescence spectrum are obtained analytically. These quantities along with the surface-induced phase-decay constant of the adatom show strong oscillatory behavior as a function of the adatom-surface distance.

*Permanent address: Institute of Physics, Academia Sinica, Beijing (Peking), The People's Republic of China.

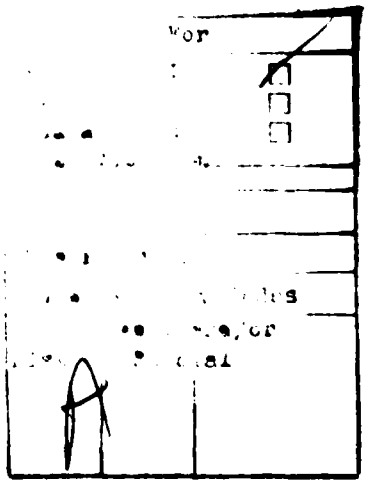

I. Introduction

Recently there has been considerable interest in the interaction of electromagnetic radiation with surfaces. The experiments which have motivated this present paper are those demonstrating the high intensity of light inelasticially scattered from molecules adsorbed on metal surfaces[1] and the surface-enhanced luminescence of an excited molecule fluorescing near or on metals and dielectric fibers.[2-4]

To investigate the basic behavior of the surface-enhanced resonance excitation of a laser-driven quantum system near or adsorbed on a surface, as a first step we calculate the resonance fluorescence spectrum of a two-level atom near or adsorbed on a metal surface. In the surface-free case, i.e., in the absence of a solid surface or when the atom is very far from the surface, resonance excitation of a two-level atom by a laser field has been extensively investigated, using the powerful optical Bloch equations.[5] There has also been interest in surface-enhanced spontaneous emission of two-level atoms near a mirror.[6-9] In this paper, we provide a derivation of the surface-dressed optical Bloch equations. The following factors are taken into account:

i) Radiative spontaneous decay and stimulated emission produced by both the driving laser field and the reflected electromagnetic field.

ii) Collisional dephasing of the two-level atom produced by foreign atoms in the gas medium, which constitutes the half region of the interface.

iii) The oscillatory behavior of the lifetime of the adatom due to interference between the driving field and the reflected field.

iv) Surface-induced dephasing of the adatomic transition dipole.

v) The interaction between the adatom and surface plasmons.

vi) The random phase fluctuation of the laser field and its influence on the spectrum.

In Section II we derive the surface-dressed optical Bloch equations. In Section III we solve the equations in the weak-field limit to obtain the population inversion and the resonance fluorescence spectrum. In Section IV we present results for these quantities and the surface-induced phase-decay constant of the adatom. Section V is the Summary.

II. Surface-Dressed Optical Bloch Equations (SBE)

Let us consider a laser-driven two-level atom near or adsorbed on a metal surface. Although the atom has no dipole moment in its ground state, it can have a significant transition dipole connecting the ground and excited states. The reflected field provided by a metallic mirror and surface plasmon resonance can influence the dynamic behavior and scattering spectrum of the adatom.

To treat this problem we utilize a self-consistent approach. This first involves the determination of the induced transition dipole by quantum mechanics, i.e., the optical Bloch equations. The transition dipole is then used in Maxwell's equations to determine the reflected field, and the reflected field in turn is used in the quantum mechanical procedure to find the transition dipole. The resulting form of the reflected field $\hat{E}_R(t)$ is

$$\hat{E}_R(t) = \mu_{12}\hat{\sigma}_{12}(t)f(d) + \mu_{21}\hat{\sigma}_{21}(t)f^*(d), \tag{1}$$

where d is the distance between the adatom and surface, μ_{ij} is the electric-dipole transition matrix element between the states $|i\rangle$ and $|j\rangle$, $\sigma_{ij} \equiv |i\rangle\langle j|$ is the adatomic transition operator, and f(d) is a distance-dependent function which will be discussed in more detail later. The SBE in operator form are then given by (assuming the equilibrium condition $\hat{W} = -1$)

$$\frac{\partial}{\partial t}\hat{\sigma}_{21}(t) = (i\omega_{21}-\gamma_2)\hat{\sigma}_{21}(t) + i\frac{\mu_{21}}{\hbar}\hat{W}\{\hat{E}(t) + [f(d)\mu_{12}\hat{\sigma}_{12}(t) + f^*(d)\mu_{21}\hat{\sigma}_{21}(t)]\} \tag{2}$$

$$\frac{\partial}{\partial t}\hat{W}(t) = -\gamma[1+\hat{W}(t)] + 2i\frac{\mu_{21}}{\hbar}\hat{\sigma}_{21}\{\hat{E}(t) + [f(d)\mu_{12}\hat{\sigma}_{12}(t) + f^*(d)\mu_{21}\hat{\sigma}_{21}(t)]\} - 2i\frac{\mu_{12}}{\hbar}\hat{\sigma}_{12}\{\hat{E}(t) + [f(d)\mu_{12}\hat{\sigma}_{12}(t) + f^*(d)\mu_{21}\hat{\sigma}_{21}(t)]\} \tag{3}$$

$$\frac{\partial}{\partial t}\hat{\sigma}_{12}(t) = \frac{\partial}{\partial t}\hat{\sigma}_{21}^{\dagger}(t), \tag{4}$$

where ω_{21} is the adatomic transition frequency, $\hat{E}(t)$ is the random phase-fluctuating electric field strength operator, γ_1 is the population relaxation constant, γ_2 is the phase relaxation constant, and $\hat{W}(t) \equiv \hat{\sigma}_{22}(t) - \hat{\sigma}_{11}(t)$ is the population inversion of the adatom. Collisions of the adatom with other atoms in the gas medium are accounted for in the impact limit by assuming $\gamma_1 \neq 2\gamma_2$.

The quantum equations of motion for $\hat{W}$, $\hat{\sigma}_{12}$ and $\hat{\sigma}_{21}$ are most useful in the rotating-wave approximation (RWA). By defining

$$\hat{S}_{12}(t) \equiv \hat{\sigma}_{12}(t)e^{i\omega_L t} \tag{5}$$

$$\hat{S}_{21}(t) \equiv \hat{\sigma}_{21}(t)e^{-i\omega_L t}, \tag{6}$$

where ω_L is the laser frequency, we can rewrite Eq. (2.2) within the RWA as

$$\frac{d}{dt}\begin{pmatrix}\hat{S}_{21}(t)\\ \hat{W}(t)\\ \hat{S}_{12}(t)\end{pmatrix} = \begin{pmatrix}-\tilde{\gamma}_2+i\Delta & i\Omega^-(t)/2 & 0\\ i\Omega^+(t) & -\gamma_1 & -i\Omega^-(t)\\ 0 & -i\Omega^+(t)/2 & -\tilde{\gamma}_2-i\Delta\end{pmatrix}\begin{pmatrix}\hat{S}_{21}(t)\\ \hat{W}(t)\\ \hat{S}_{12}(t)\end{pmatrix}$$

$$-\gamma_1\begin{pmatrix}0\\1\\0\end{pmatrix}. \tag{7}$$

$\Omega^{\pm}(t) \equiv \Omega\exp[\mp i\phi(t)]$ is the time-dependent Rabi frequency, where $\Omega \equiv \frac{2}{\hbar}|\mu_{21}|E_0(t)$ and $E(t)$ is written as an expectation value in a coherent state of the laser field in terms of the phase factor $\phi(t)$ as $E(t) = E_0(t)\exp[-i\omega_L t + i\phi(t)] + c.c.$; $\Delta \equiv \omega_{21} - \omega_L$ is the detuning; the surface-induced phase-decay constant is $\gamma_\Delta \equiv \frac{2}{\hbar}\,\mathrm{Im}(f)|\mu_{12}|^2$; and $\tilde{\gamma}_2 = \gamma_2 + \gamma_\Delta$.

To calculate γ_Δ, we must know the reflected field [Eq. (1)] or the complex function $f(d)$, which can be determined by the Sommerfeld-Hertz vector procedure.[2] For the case of a laser-excited atom emitting near a metallic half space, the imaginary part of $f(d)$ has the following form:

$$\mathrm{Im}(f) = \frac{\zeta}{1+\epsilon_1^2} \frac{k_1^3}{\left[\omega^2 - \frac{\omega_p^2}{1+\epsilon_1}\right]^2 + \frac{\delta^2\omega_p^4}{(1+\epsilon_1)^2\omega^2}}$$

$$\times \{\frac{1}{\epsilon_1}[(\omega^2-\omega_p^2)^2 + \frac{\omega_p^4\delta^2}{\omega^2} - \epsilon_1^2\omega^4][\eta \sin D - \frac{1}{D^2}\cos D]$$

$$+ 2\omega\delta\omega_p^2[\eta \cos D + \frac{1}{D^2}\sin D]\}, \qquad (8)$$

where $\zeta = 1$ and $\eta \equiv \frac{1}{D^3} + \frac{1}{D}$ for the case of the induced dipole oriented parallel to the surface, $\zeta = 2$ and $\eta \equiv \frac{1}{D^3}$ for the perpendicular case, ϵ_1 is the dielectric constant for the gas medium, $k_1 = \omega\sqrt{\epsilon_1}/c$ is the wave number, ω is the emission frequency, c is the speed of light, and $D = 2k_1 d$ is the reduced distance which is dimensionless. The Drude model[10] has been used to determine the dielectric constant of the metal medium, i.e.,

$$\epsilon_2(\omega) = 1 - \frac{\omega_p^2}{\omega(\omega + i\delta)}, \qquad (9)$$

where δ is the inverse of the relaxation time and ω_p is the plasma frequency. We note that Im(f) has a resonance at $\omega_{sp} = \omega_p(1 + \epsilon_1)^{-1/2}$, which is the surface plasmon frequency of the interface, so that the reflected field given by Eq. (1) involves resonance energy transfer between the adatom and the excited surface plasmon.

Eq. (8) leads to a surface-induced phase-decay constant (in the unit of Einstein's spontaneous decay constant $A \equiv \frac{4\omega_{21}^3}{3\hbar c}|\mu_{21}|^2$) of the following form:

$$\gamma_\delta = \zeta a_0[a_1(\eta \sin D - \frac{\cos D}{D^2}) + a_2(\eta \cos D + \frac{\sin D}{D^2})], \tag{10}$$

where

$$a_0 = \frac{3}{8}\frac{1}{(1-\beta^2)^2 + (\alpha/\omega_{\delta p})^2} \tag{11}$$

$$a_1 = (2-\beta^2)^2 + (2\alpha/\omega_{\delta p})^2 - \beta^4 \tag{12}$$

$$a_2 = (2\beta)^2\alpha/\omega_{\delta p}. \tag{13}$$

$\beta \equiv \omega_L/\omega_{\delta p}$, $\alpha \equiv \delta/\beta$, ζ and η are the same as in Eq. (8) for the parallel and perpendicular cases, and $\epsilon_1 = 1$ has been assumed so that $\omega_{\delta p} = \omega_p/\sqrt{2}$. The above expression for γ_δ can be further simplified by assuming perfect reflection, i.e., $R^\perp = R^{\parallel} = -1$, where $R^{\parallel}$ is the reflection coefficient for an incident ray polarized parallel to the plane of incidence (p-polarized) and $R^\perp$ is the reflection coefficient for perpendicular polarization (δ-polarized). Then

$$\gamma_\delta = \frac{3}{2}\zeta(\eta \sin D - \frac{\cos D}{D^2}). \tag{14}$$

III. Resonance Fluroescence Spectrum

In this section we consider the weak field or large detuning limit, where $W(t) \equiv \langle\langle\hat{W}(t)\rangle\rangle = -1$. We also use the phase-diffusion model[11,12] for the laser field in order to include the effects of the laser bandwidth γ_L:

$$\langle\langle\Omega^-(t_1)\Omega^+(t_2)\rangle\rangle = \Omega^2 e^{-\gamma_L|t_2-t_1|}. \tag{15}$$

The double bracket signifies two averages: one is over the stochastic ensemble, and the other is a standard quantum mechanical average. Eq. (15) applies to a partially-coherent laser field, which is the realistic situation. Given that the atom near the metal remains more or less in in its ground state, we can linearize Eq. (7) to obtain

$$\frac{d}{dt}\hat{S}_{21}(t) = -(\gamma_2 + \gamma_\phi - i\Delta)\hat{S}_{21}(t) - \frac{i}{2}\Omega^-(t). \tag{16}$$

To determine the population inversion, let us take the laser field to be turned on at $t = 0$ with a constant amplitude for $t \geq 0$. We then obtain the analytical form

$$W(t) = -1 + \Omega^2\{\frac{\tilde{\gamma}_2+\gamma_L}{\gamma_1[(\tilde{\gamma}_2+\gamma_L)^2+\Delta^2]} + \frac{\gamma_1-\tilde{\gamma}_2-\gamma_L}{\gamma_1[(\gamma_1-\tilde{\gamma}_2-\gamma_L)^2+\Delta^2]} e^{-\gamma_1 t}$$

$$- \frac{[(\tilde{\gamma}_2+\gamma_L)(\gamma_1-\tilde{\gamma}_2-\gamma_L) + \Delta^2]\cos(\Delta t) + \Delta(2\tilde{\gamma}_2-2\gamma_L-\gamma_1)\sin(\Delta t)}{[(\tilde{\gamma}_2+\gamma_L)^2+\Delta^2][(\gamma_1-\tilde{\gamma}_2-\gamma_L)^2 + \Delta^2]}$$

$$\times e^{-(\tilde{\gamma}_2 + \gamma_L)t}\}. \tag{17}$$

To obtain the power spectrum of the scattered light, we must find the dipole-dipole correlation function $\langle\langle\hat{S}_{21}(t_2)\hat{S}_{12}(t_1)\rangle\rangle$. For $t_1, t_2 >> \gamma_1^{-1}, \gamma_2^{-1}$ this takes the form ($t_2 \geq t_1$)

$$\langle\langle\hat{S}_{21}(t_2)\hat{S}_{12}(t_1)\rangle\rangle = \frac{\Omega}{4}\frac{1}{(\tilde{\gamma}_2+\gamma_L)+i\Delta}$$

$$\times \frac{2(\tilde{\gamma}_2+\gamma_L)(\tilde{\gamma}_2-\gamma_L-i\Delta)-\gamma_1[(\tilde{\gamma}_2+\gamma_L)-i\Delta]}{\gamma_1(\tilde{\gamma}_2+\gamma_L-i\Delta)(\tilde{\gamma}_2-\gamma_L-i\Delta)} e^{-(\tilde{\gamma}_2-i\Delta)(t_2-t_1)}$$

(continued)

(continued)

$$+ \frac{\Omega^2}{4} \frac{e^{-\gamma_L(t_2-t_1)}}{(\tilde{\gamma}_2+\gamma_L+i\Delta)(\tilde{\gamma}_2-\gamma_L-i\Delta)} \cdot \tag{18}$$

The corresponding power spectrum for the emitted frequency ω is given by the Fourier transform of the above equation:

$$S(\omega) = \frac{\Omega^2}{2} \frac{1}{(\tilde{\gamma}_2+\gamma_L)^2+\Delta^2} \{ \frac{1}{(\tilde{\gamma}_2-\gamma_L)^2+\Delta^2} [\frac{\gamma_L(\tilde{\gamma}_2^2-\gamma_L^2+\Delta^2) + 2\gamma_L\Delta(\omega-\omega_L)}{\gamma_L^2 + (\omega-\omega_L)^2}$$

$$- \frac{\tilde{\gamma}_2(\tilde{\gamma}_2^2-\gamma_L^2+\Delta^2) + 2\gamma_L\Delta(\omega-\omega_{21})}{\tilde{\gamma}_2^2 + (\omega-\omega_{21})^2}] + \frac{2(\tilde{\gamma}_2+\gamma_L)\tilde{\gamma}_2}{\gamma_1[\tilde{\gamma}_2^2 + (\omega-\omega_{21})^2]}\} \tag{19}$$

The fluorescence spectrum of Eq. (19) generally exhibits two peaks for a surface-dressed two-level atom in a weak, partially-coherent laser field. One peak is centered at $\omega = \omega_L$, which corresponds to elastic or Rayleigh scattering, and the other near $\omega = \omega_{21}$ corresponds to inelastic scattering or fluorescence. In the surface-free case for a collisionless atom in a fully-coherent laser field ($\gamma_1 = 2\gamma_2 = A$, $\gamma_L = 0$), the above spectrum becomes a single peak,

$$S(\omega) = \frac{\pi\Omega^2/2}{(A/2)^2+\Delta^2} \delta(\omega-\omega_L), \tag{20}$$

which is the standard result of Heitler.[13] In general, however, the adatom suffers collisions with foreign atoms in the gas medium, so that $\gamma \neq 2\gamma_2$, and there are nonzero values for the surface-induced phase-decay constant γ_δ and the laser bandwidth γ_L. This is then responsible for the second Lorentzian peak occurring near the transition frequency ω_{21}.

IV. Results

Fig. 1 shows the time evolution of the population inversion W(t) [Eq. (17)] for an atom near a metal surface for two different adatom-surface plasmon resonance conditions, $\beta \equiv \omega_L/\omega_{\delta p} = 0.5$ and $\beta = 0.9$. We have used the value of 3.5×10^{-3} for the ratio $\delta/\omega_{\delta p}$, which corresponds to a silver surface. Each curve approaches a stationary-state value, assuming that the duration of the laser pulse is much longer than the relaxation time of the adatom (characterized by γ_1^{-1} and $\tilde{\gamma}_2^{-1}$). The reason the values of W for the off-resonance case ($\beta = 0.5$) are less than those for the near-resonance case ($\beta = 0.9$) is that the levels of the adatom in the latter case are strongly broadened by the resonant transfer of energy between the adatom and surface plasmon, so that the population of the upper level increases. The oscillations increase and the damping due to the reflected field disappears as the adatom moves further from the surface (going from curve 1 to 3). The strong oscillations in the nearly surface-free case (curve 3) are caused by beating between the driving laser field and the "adatomic oscillator".

Fig. 2 displays the resonance fluorescence spectrum [Eq. (19)], with the Rayleigh and fluorescence peaks. The former peak in our

model is just determined by the laser bandwidth γ_L. The latter peak is strongly dependent on the adatom-surface distance; as the distance decreases, the upper adatomic level broadens and hence the fluroescence intensity increases.

In Fig. 3 we plot W(t) for the case of a perfectly reflective metal surface, $R^{\perp} = R^{\parallel} = -1$ [see Eq. (14)], for several values of the laser bandwidth and adatom-surface distance. The oscillations increase as the adatom moves further from the surface and decrease as the laser bandwidth increases [going from (a) to (c)]. A larger bandwidth leads to more damping of the adatomic oscillator [see Eq. (17)] and hence an increase in the population inversion. It is interesting to note that W is more sensitive to the adatom-surface distance for the case of the transition dipole oriented parallel to the surface than for the perpendicular case. We see that the positions of the dashed curves 2 and 3 are interchanged, indicating that the power spectrum oscillates as a function of D. As seen by the form of Eq. (8), we would also see such oscillations for the population inversion and power spectrum in Figs. 1 and 2 if we were to consider a wider range of values of D.

Fig. 4 displays the surface-induced phase-decay constant γ_Δ as a function of the adatom-surface distance for a perfectly reflective surface. The oscillations are due to the interference between the reflected field and the driving field. This gives rise to oscillations in the lifetime of the adatomic oscillator, while the small negative value of γ_Δ in some regions of D tends to increase the lifetime.

Fig. 5 shows the power spectrum for several values of the laser bandwidth γ_L. When γ_L is very small compared to the phase-decay constant γ_2 [Fig. 5(a)],

the power is concentrated largely in the Rayleigh peak. Here the population of the upper adatomic level, and hence the power of the fluorescence, is determined mainly by the broadening of that level due to the surface, so that the power increases as D decreases. The situation is changed when γ_L is larger than γ_2, in which case the power of the Rayleigh component transfers to the fluorescence peak [Fig. 5(b) and (c)]. Although a decrease in D leads to a broadening of the adatomic level, now the total power in the fluorescence peak is approximately unchanged, whereby a curve for smaller D has a larger width but a smaller peak height. A more detailed discussion on the relation between fluorescence and laser bandwidth in general will be published later.

It is interesting to note that Weitz et al recently published measurements and a theoretical model on a hierarchy of enhancement ratios for normal Raman scattering, resonance Raman scattering and fluorescence from molecules adsorbed on a silver surface.[14] The results from our two-level adatom model for surface-enhanced fluorescence are in good agreement with their measured enhancement ratio of 10^{-1} to 10 for fluorescence.

V. Summary

A simple model has been developed to describe the dynamic behavior of a two-level adatom at a metal surface. Surface-dressed optical Bloch equations (SBE), which account for surface-reflected photons and adatom-surface plasmon coupling, have been derived. Collisions with foreign gas atoms and effects of the laser bandwidth have been included. The SBE have been used to evaluate the power spectrum of the scattered light, the population inversion and the surface-induced phase-decay constant as functions of the adatom-surface distance and adatom-surface plasmon resonance parameter β. The displayed properties of the laser-adatom-surface system should be useful in understanding basic processes occurring in surface resonance spectroscopy.

Acknowledgments

This work was supported in part by the Office of Naval Research, the Air Force Office of Scientific Research (AFSC) under Grant No. AFOSR 82-0046 and the U.S. Army Research Office. The United States Government is authorized to reproduce and distribute reprints for governmental purposes notwithstanding any copyright notation hereon. TFG acknowledges the Camille and Henry Dreyfus Foundation for a Teacher-Scholar Award (1975-84) and the John Simon Guggenheim Memorial Foundation for a Fellowship (1983-84). XYH acknowledges helpful conversations with Professors S. Mukamel, L. Mandel and P. W. Milonni.

References

1. See, for example the review article by T. E. Furtak and J. Reyes, Surface Sci. 93, 351 (1980), and the references contained therein.
2. See the review by R. R. Chance, A. Prock and R. Silbey, Adv. Chem. Phys. 37, 1 (1978).
3. A. M. Glass, P. F. Liao, J. G. Bergman and D. H. Olson, Opt. Lett. 5, 368 (1980).
4. J. F. Owen, P. W. Barber, P. B. Dorain and R. K. Chang, Phys. Rev. Lett. 47, 1075 (1981).
5. L. Allen and J. H. Eberly, Optical Resonance and Two-Level Atoms (Wiley, New York, 1975).
6. V. L. Lyuboshitz, Soviet Physics JETP 26, 937 (1968).
7. H. Morawitz, Phys. Rev. 187, 1972 (1969).
8. P. W. Milonni and P. L. Knight, Opt. Commun. 9, 119 (1973).
9. G. S. Agarwal, Opt. Commun. 42, 205 (1982).

10. M. Born and W. Wolf, Principles of Optics (Pergamon, New York, 1975) pp. 624-627.

11. R. J. Glauber, in Quantum Optics and Electronics, edited by C. DeWitt A. Blandin and C. Cohen-Tannoudji (Gordon and Breach, New York, 1965), pp. 65-185.

12. J. H. Eberly, Phys. Rev. Lett. 37, 1387 (1976).

13. W. Heitler, The Quantum Theory of Radiation (Oxford, London, 1954).

14. J. H. Eberly, X. Y. Huang and G. S. Agarwal, to be published.

15. D. A. Weitz, S. Garoff, J. I. Gersten and A. Nitzan, J. Chem. Phys. 78, 5324 (1983).

Figure Captions

1. Time evolution of the population inversion in the weak field or large detuning limit, with $(\gamma_L, \Omega, \Delta) = (0.3, 0.05, 5)$ in the unit A for $\beta = 0.9$ (solid curves) and $\beta = 0.5$ (dashed curves). Curves 1, 2 and 3 correspond to the values of the reduced distance $D = 2k_1 d$ of 1, 3 and 5, respectively. The horizontal axis corresponds to time in the unit A^{-1}. The quantity $[W(t) + 1]/\Omega^2$ is shown along the vertical axis.

2. Fluorescence power spectrum of scattered light with $(\gamma_L, \Omega, \Delta) = (0.3, 0.05, 5)$ in the unit A and $\beta = 0.9$ for the induced transition dipole oriented perpendicular to the surface. The units along the vertical axis are arbitrary. Curves 1, 2 and 3 correspond to D = 1, 3 and 5, respectively.

3. Time evolution of the population inversion W(t) of an adatom at a perfectly reflective metal surface, with $\Omega = 0.05$, $\Delta = 5$, (a) $\gamma_L = 0.3$, (b) $\gamma_L = 1$, and (c) $\gamma_L = 3$ (in the unit A). The solid curves are for the induced transition dipole oriented perpendicular to the surface, while the dashed curves are for the parallel case, and the labels 1, 2 and 3 correspond to D = 2, 4 and 6, respectively.

4. Surface-induced phase-decay constant γ_Δ (in the unit A) as a function of the reduced adatom-surface distance $D = 2k_1 d$ for a perfectly reflective metal surface. The solid curve is for the induced transition dipole oriented perpendicular to the surface, while the dashed curve is for the parallel case.

5. Power spectrum of scattered light for a perfectly reflective metal surface, with $\Omega = 0.05$, $\Delta = 5$, (a) $\gamma_L = 0.3$, (b) $\gamma_L = 1$ and (c) $\gamma_L = 3$ (in the unit A). The induced transition dipole is oriented perpendicular to the surface. The units along the vertical axis are arbitrary. Curves 1, 2 and 3 correspond to D = 2, 4 and 6, respectively.

Fig. 1

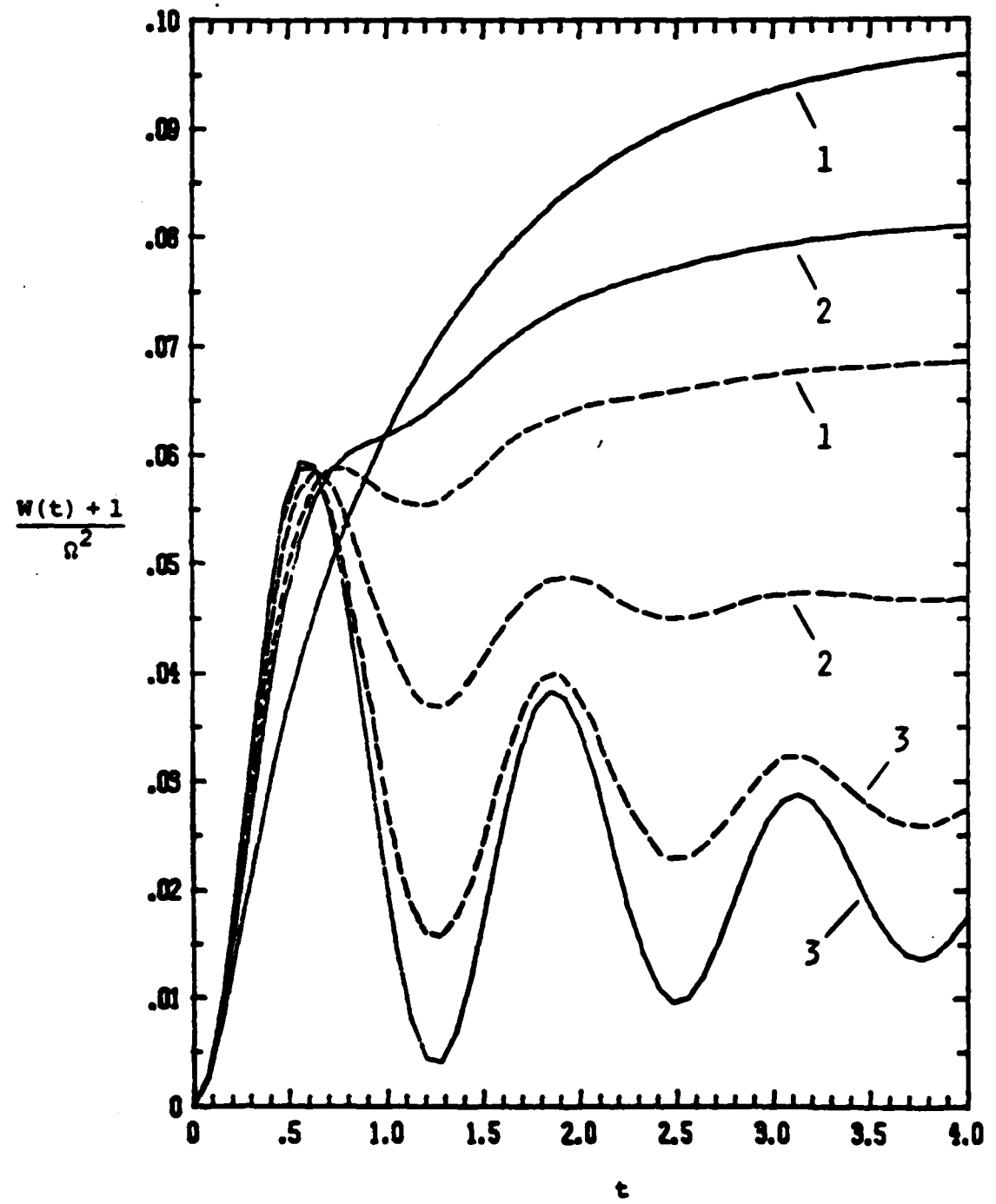

Fig. 2

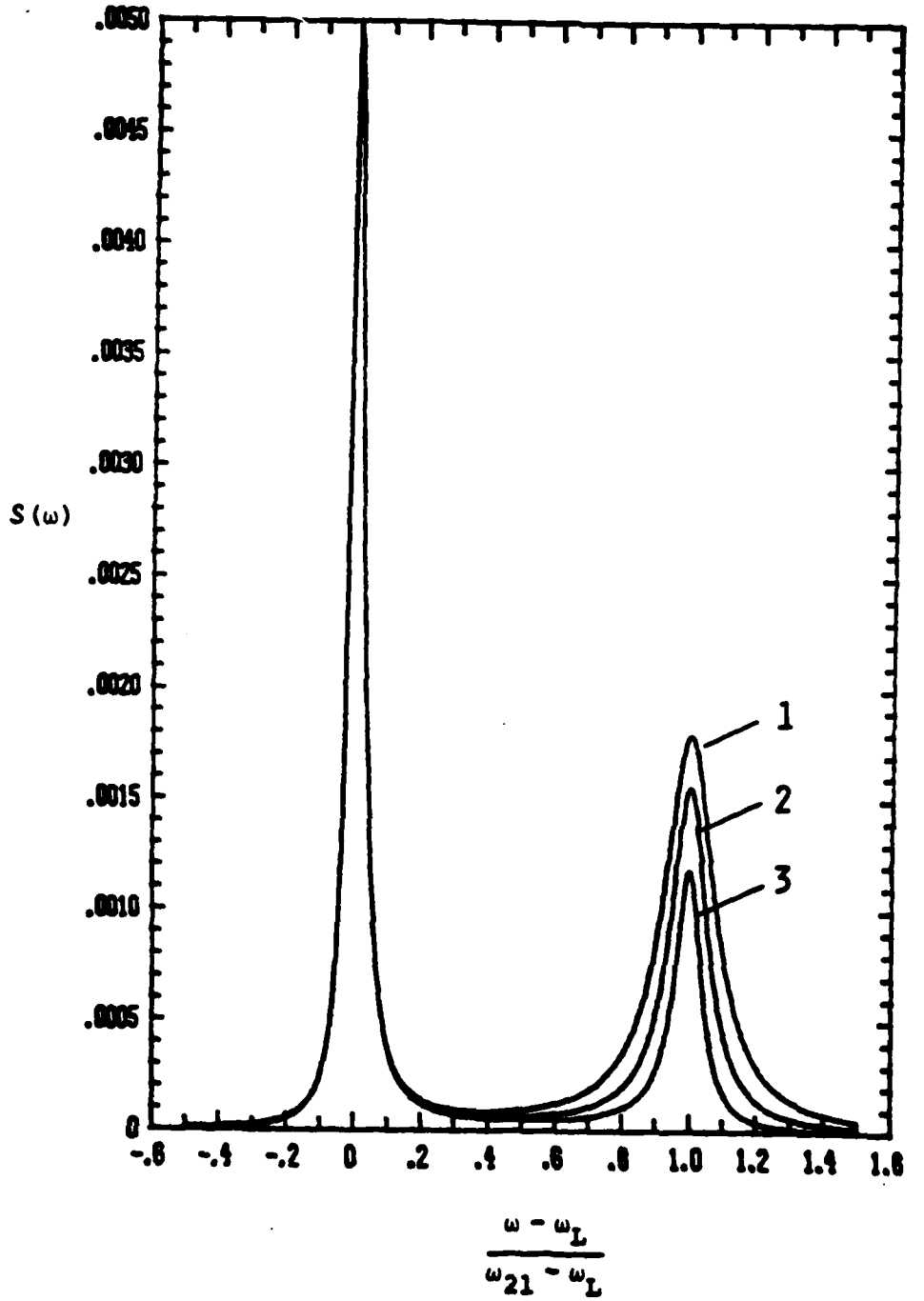
.0050
.0045
.0040
.0035
.0030
.0025
.0020
.0015
.0010
.0005
0
S(ω)
-.6
-.4
-.2
0
.2
.4
.6
.8
1.0
1.2
1.4
1.6
1
2
3
$\frac{\omega - \omega_L}{\omega_{21} - \omega_L}$

Fig. 3(a)

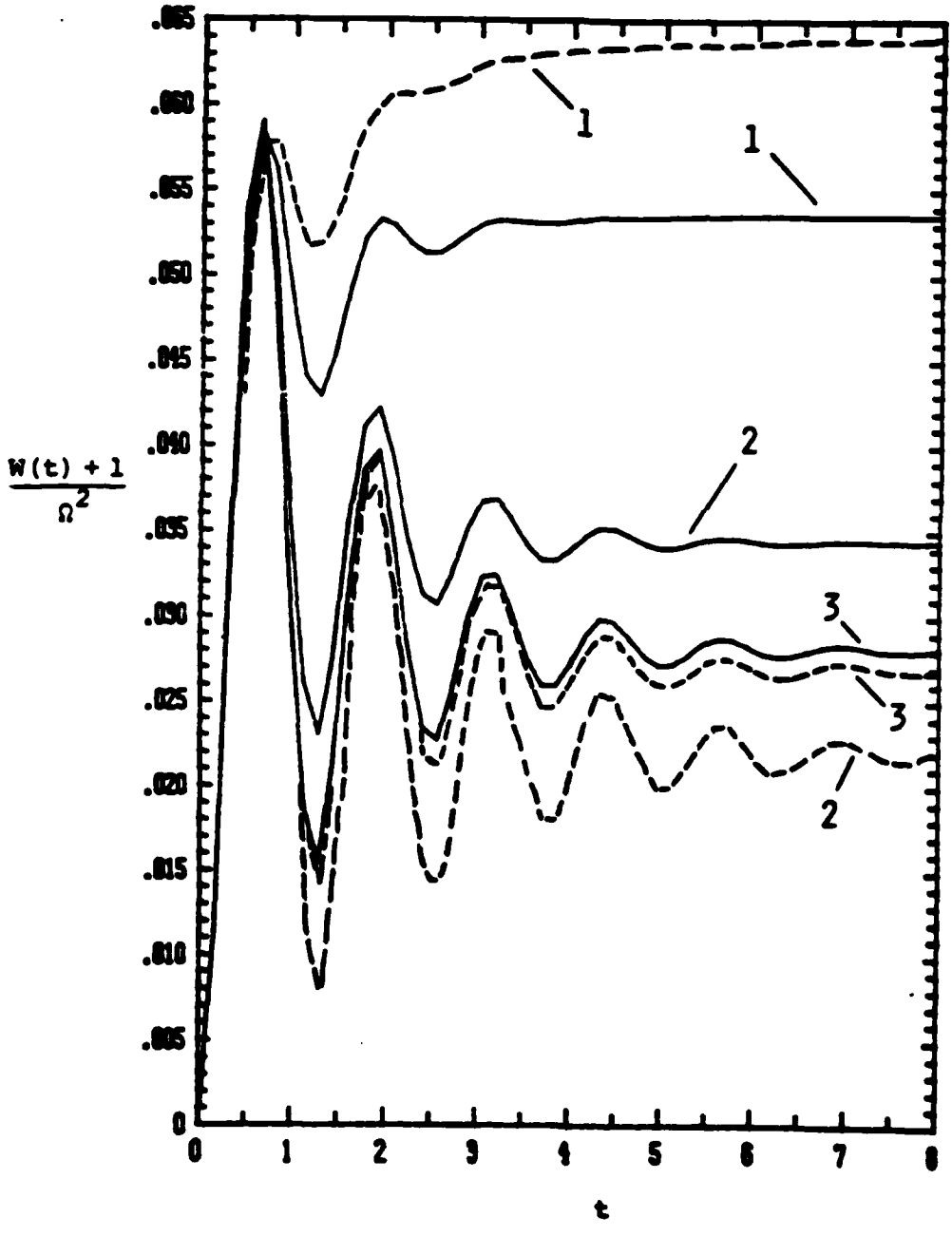
W(t) + 1
Ω²
.065
.060
.055
.050
.045
.040
.035
.030
.025
.020
.015
.010
.005
0
0
1
2
3
4
5
6
7
8
t
1
1
2
3
3
2

Fig. 3(b)

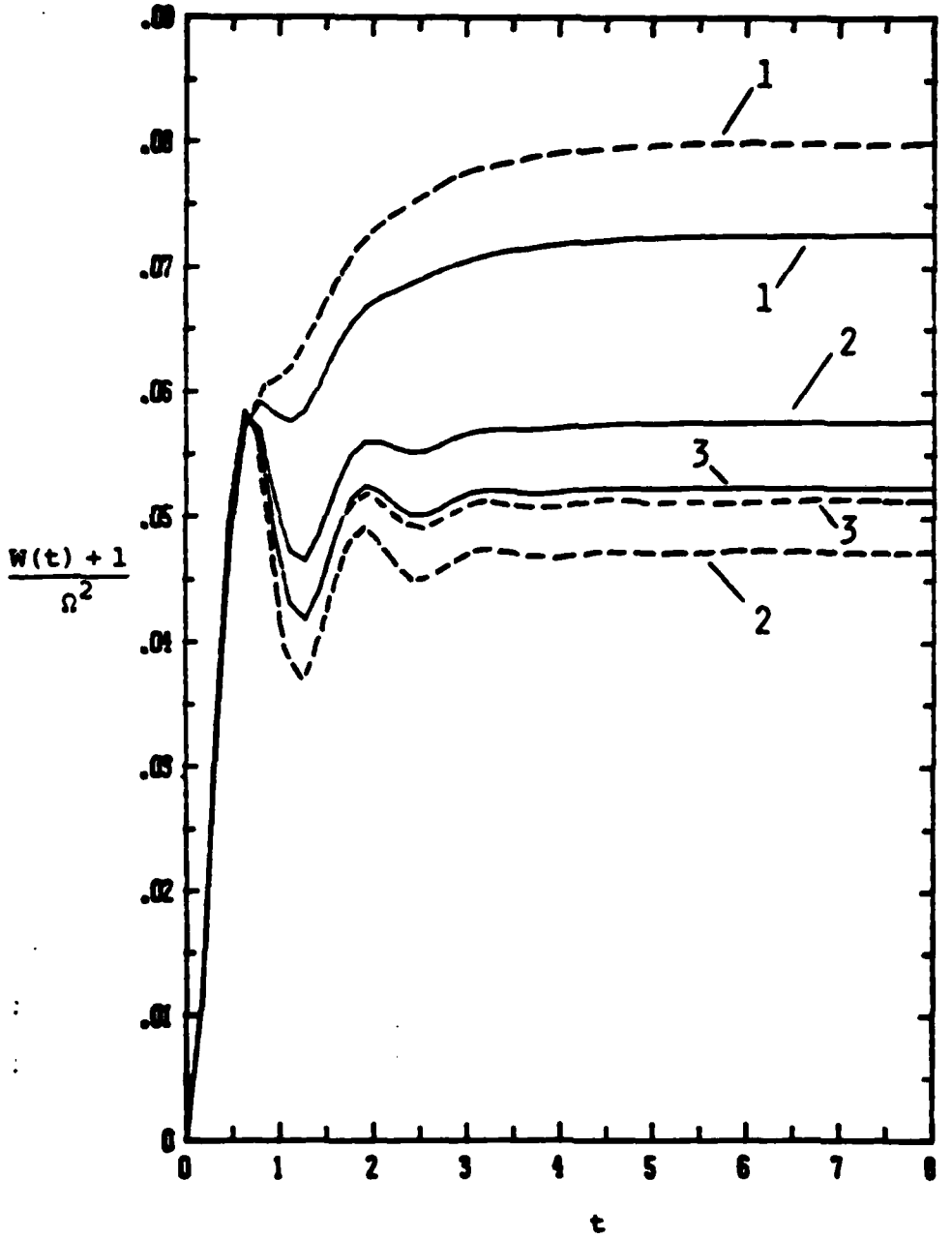

Fig. 3(c)

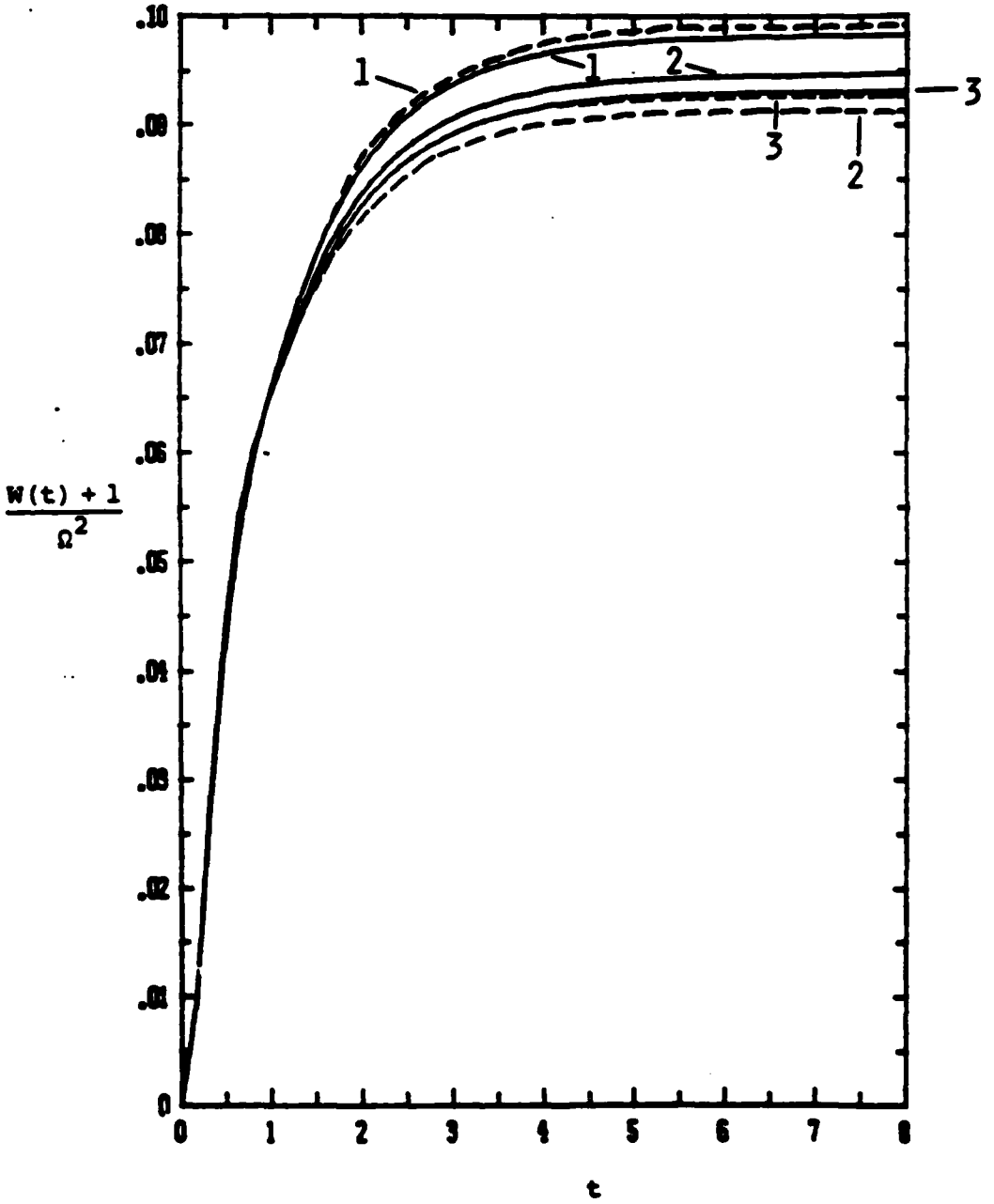

Fig. 4

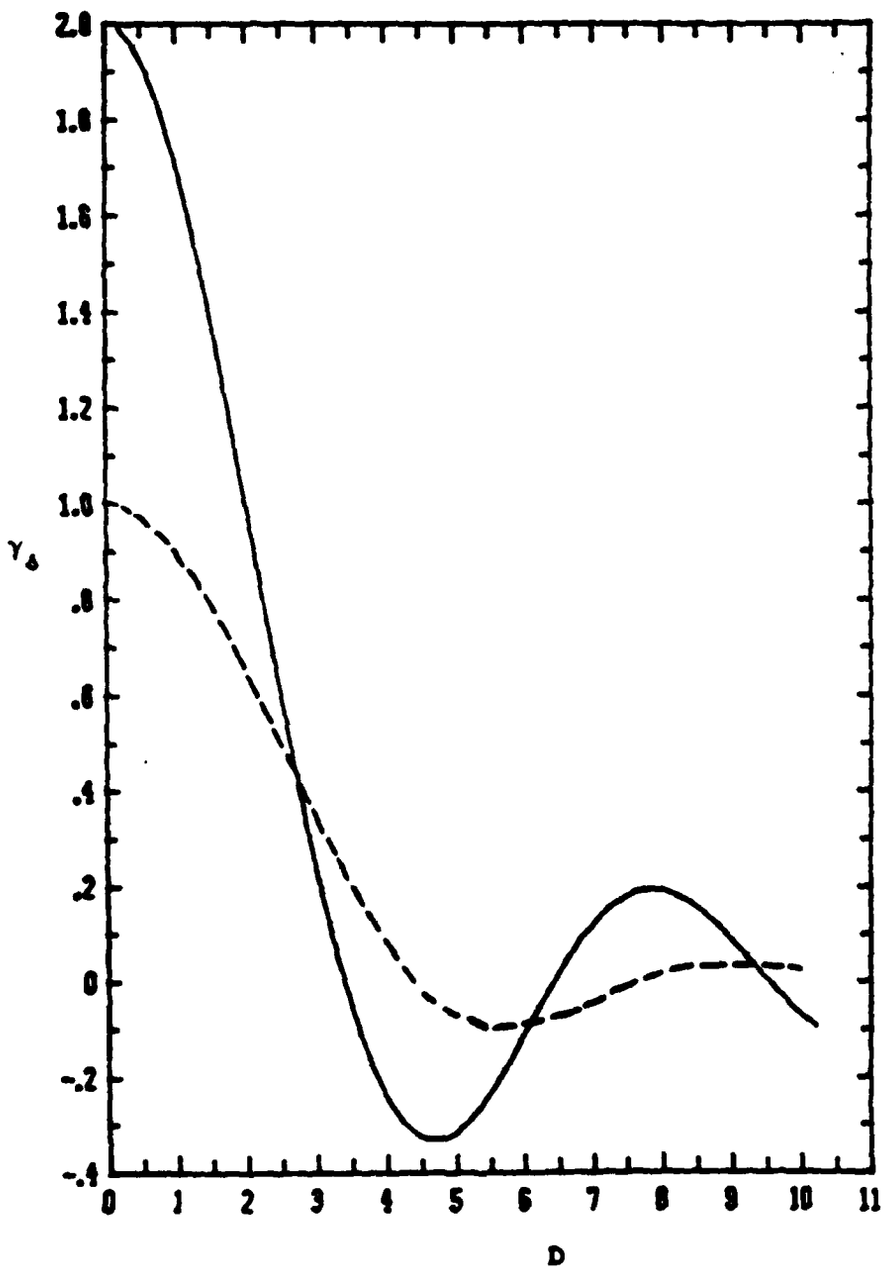

Fig. 5(a)

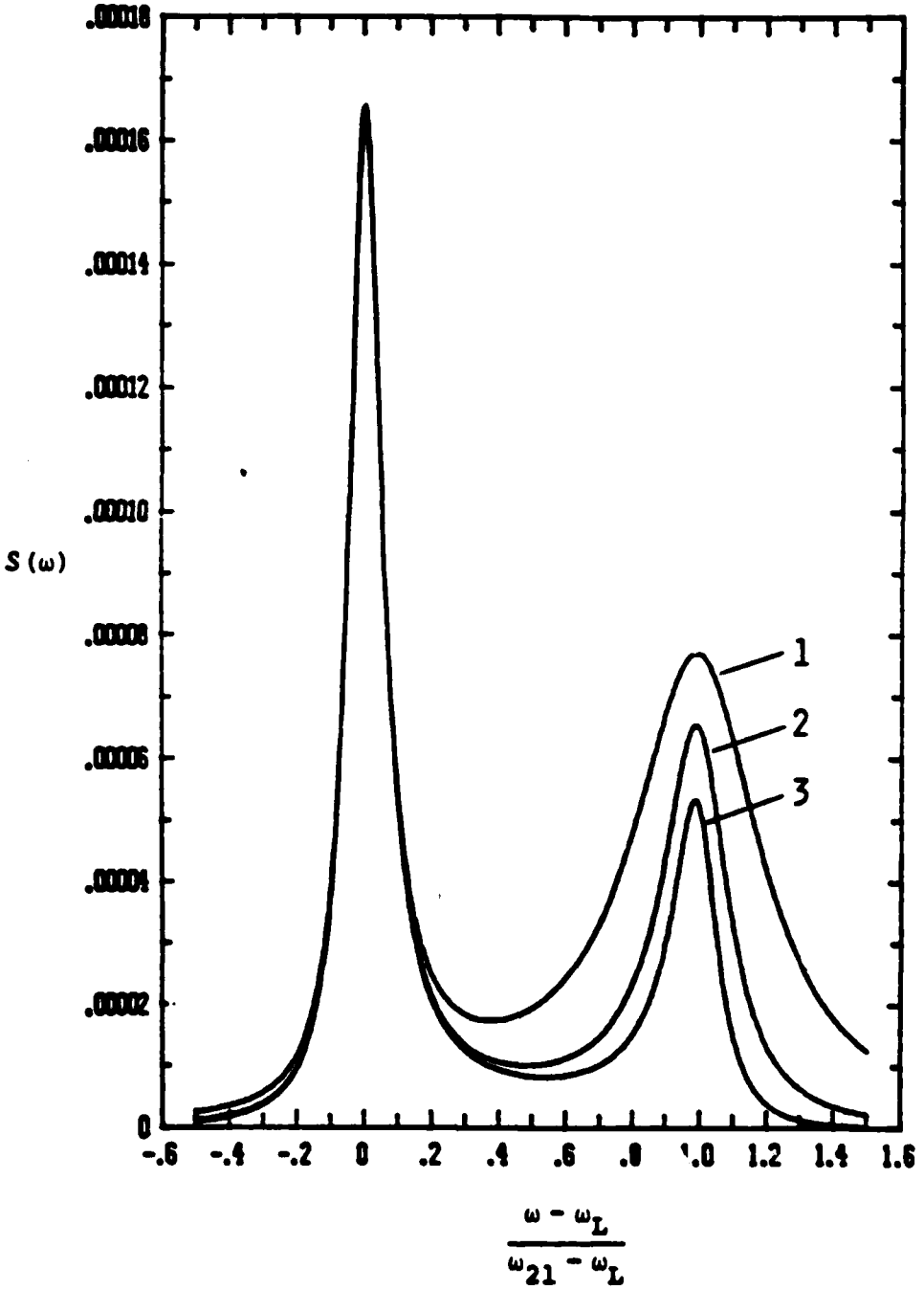
.00018
.00016
.00014
.00012
.00010
.00008
.00006
.00004
.00002
0
S(ω)
-.6
-.4
-.2
0
.2
.4
.6
.8
1.0
1.2
1.4
1.6
1
2
3
$\frac{\omega - \omega_L}{\omega_{21} - \omega_L}$

Fig. 5 (b)

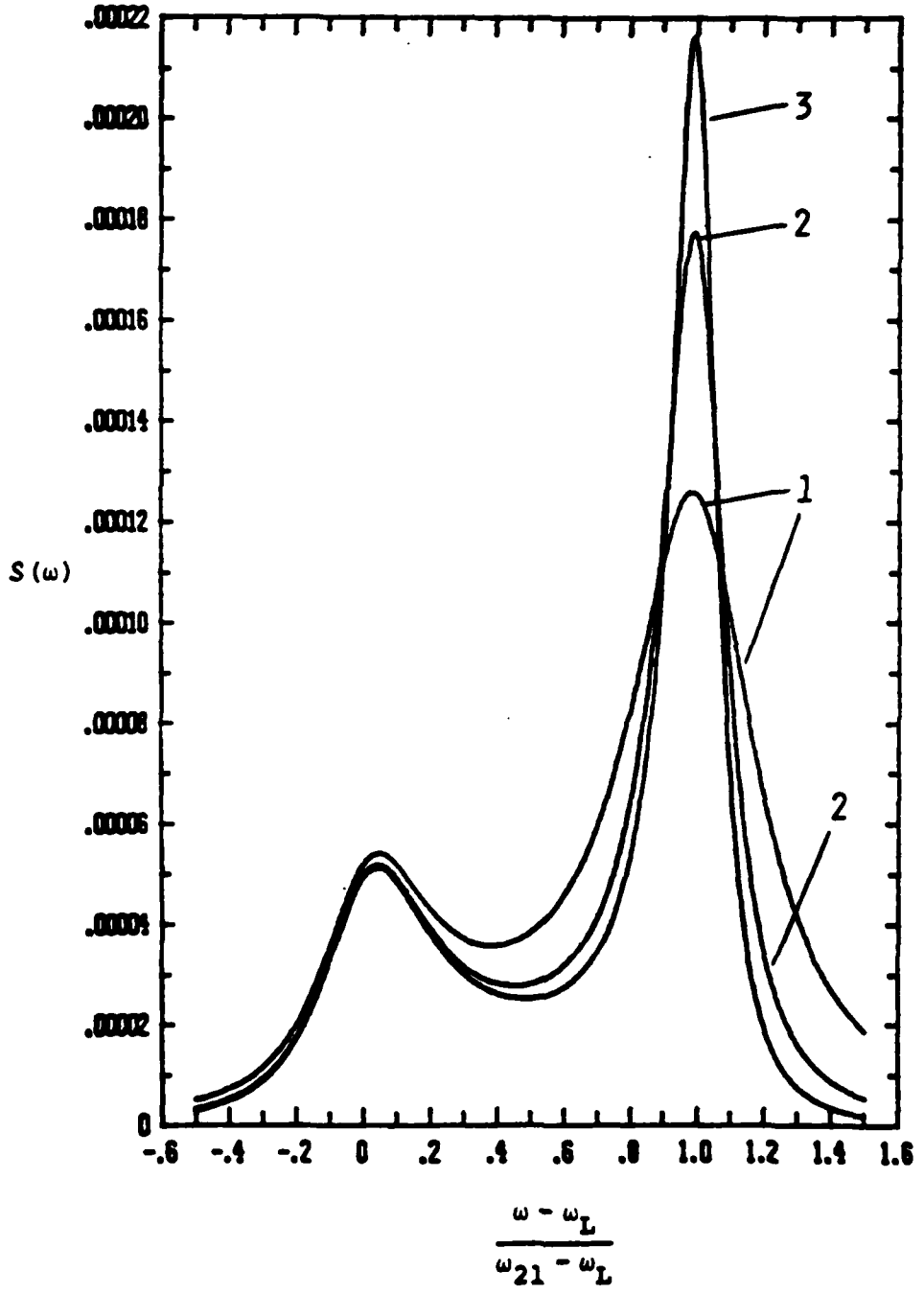
.00022
.00020
.00018
.00016
.00014
.00012
.00010
.00008
.00006
.00004
.00002
0
S (ω)
-.6
-.4
-.2
0
.2
.4
.6
.8
1.0
1.2
1.4
1.6
3
2
1
2
$\frac{\omega - \omega_L}{\omega_{21} - \omega_L}$

Fig. 5(c)

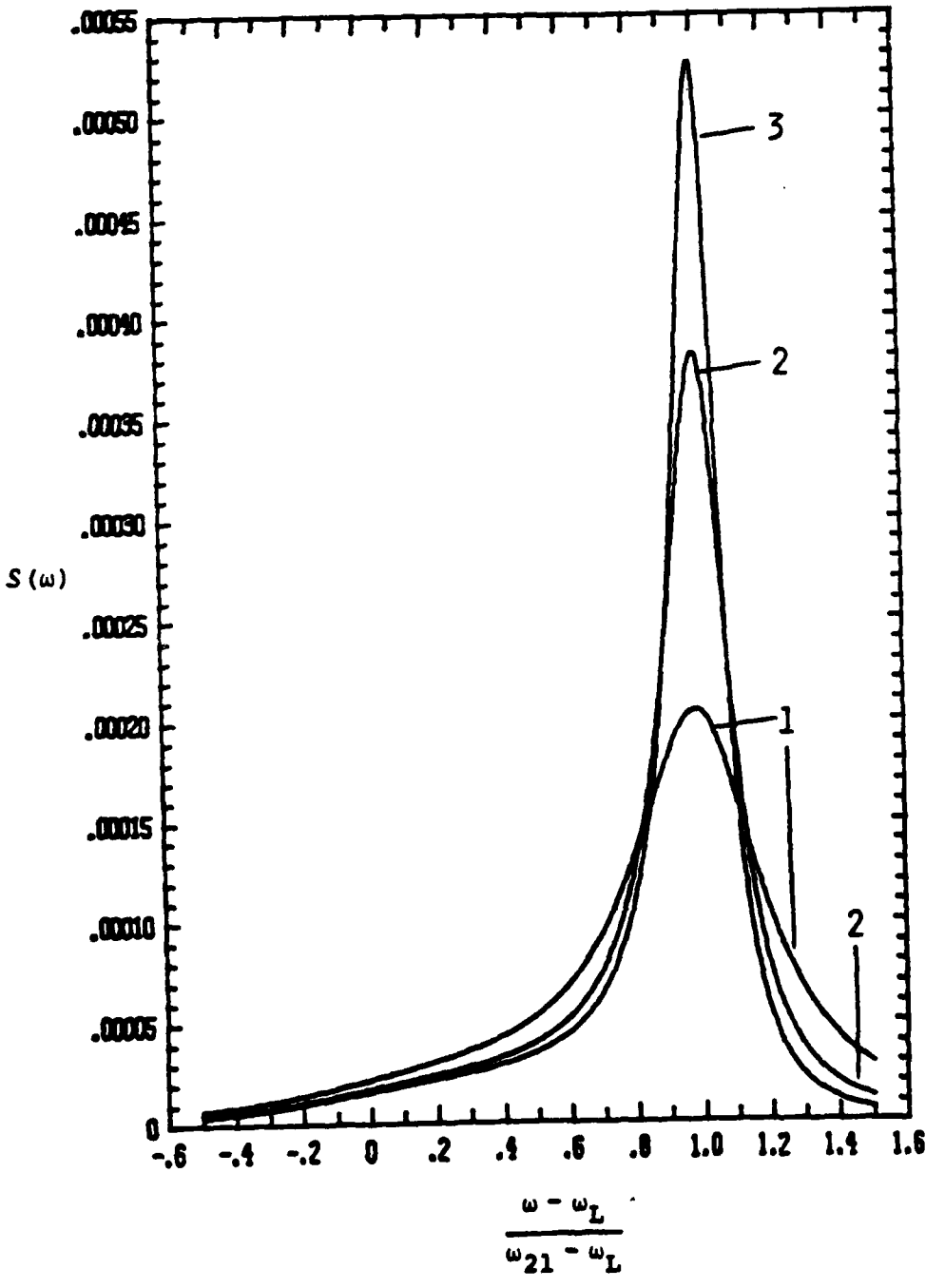
.00055
.00050
.00045
.00040
.00035
.00030
.00025
.00020
.00015
.00010
.00005
0
S(ω)
3
2
1
2
-.6
-.4
-.2
0
.2
.4
.6
.8
1.0
1.2
1.4
1.6
ω - ω_L / ω_21 - ω_L

472:GAN:716-4
94/GEN

TECHNICAL REPORT DISTRIBUTION LIST, GEN

	No. Copies
Office of Naval Research Attn: Code 413 800 North Quincy Street Arlington, Virginia 22217	2
ONR Pasadena Detachment Attn: Dr. R. J. Marcus 1030 East Green Street Pasadena, California 91106	1
Commander, Naval Air Systems Command Attn: Code 310C (H. Rosenwasser) Department of the Navy Washington, D.C. 20360	1
Defense Technical Information Center Building 5, Cameron Station Alexandria, Virginia 22314	12
Dr. Fred Saalfeld Chemistry Division, Code 6100 Naval Research Laboratory Washington, D.C. 20375	1
U.S. Army Research Office Attn: CRD-AA-IP P. O. Box 12211 Research Triangle Park, N.C. 27709	1
Mr. Vincent Schaper DTNSRDC Code 2803 Annapolis, Maryland 21402	1
Naval Ocean Systems Center Attn: Dr. S. Yamamoto Marine Sciences Division San Diego, California 91232	1
Dr. David L. Nelson Chemistry Program Office of Naval Research 800 North Quincy Street Arlington, Virginia 22217	1
Naval Ocean Systems Center Attn: Mr. Joe McCartney San Diego, California 92152	1
Naval Weapons Center Attn: Dr. A. B. Amster, Chemistry Division China Lake, California 93555	1
Naval Civil Engineering Laboratory Attn: Dr. R. W. Drisko Port Hueneme, California 93401	1
Dean William Tolles Naval Postgraduate School Monterey, California 93940	1
Scientific Advisor Commandant of the Marine Corps (Code RD-1) Washington, D.C. 20380	1
Naval Ship Research and Development Center Attn: Dr. G. Bosmajian, Applied Chemistry Division Annapolis, Maryland 21401	1
Mr. John Boyle Materials Branch Naval Ship Engineering Center Philadelphia, Pennsylvania 19112	1
Mr. A. M. Anzalone Administrative Librarian PLASTEC/ARRADCOM Bldg 3401 Dover, New Jersey 07801	1

TECHNICAL REPORT DISTRIBUTION LIST, 056

	No. Copies
Dr. G. A. Somorjai Department of Chemistry University of California Berkeley, California 94720	1
Dr. J. Murday Naval Research Laboratory Surface Chemistry Division (6170) 455 Overlook Avenue, S.W. Washington, D.C. 20375	1
Dr. J. B. Hudson Materials Division Rensselaer Polytechnic Institute Troy, New York 12181	1
Dr. Theodore E. Madey Surface Chemistry Section Department of Commerce National Bureau of Standards Washington, D.C. 20234	1
Dr. J. M. White Department of Chemistry University of Texas Austin, Texas 78712	1
Dr. Keith H. Johnson Department of Metallurgy and Materials Science Massachusetts Institute of Technology Cambridge, Massachusetts 02139	1
Dr. J. E. Demuth IBM Corporation Thomas J. Watson Research Center P. O. Box 218 Yorktown Heights, New York 10598	1
Dr. C. P. Flynn Department of Physics University of Illinois Urbana, Illinois 61801	1
Dr. W. Kohn Department of Physics University of California (San Diego) La Jolla, California 92037	1
Dr. R. L. Park Director, Center of Materials Research University of Maryland College Park, Maryland 20742	1
Dr. W. T. Peria Electrical Engineering Department University of Minnesota Minneapolis, Minnesota 55455	1
Dr. Chia-wei Woo Department of Physics Northwestern University Evanston, Illinois 60201	1
Dr. Robert M. Hexter Department of Chemistry University of Minnesota Minneapolis, Minnesota 55455	1
Dr. R. P. Van Duyne Chemistry Department Northwestern University Evanston, Illinois 60201	1
Dr. S. Sibener Department of Chemistry James Franck Institute 5640 Ellis Avenue Chicago, Illinois 60637	1
Dr. M. G. Lagally Department of Metallurgical and Mining Engineering University of Wisconsin Madison, Wisconsin 53706	1

472:GAN:716-4
94/056

TECHNICAL REPORT DISTRIBUTION LIST, 056

	No. Copies
Dr. Robert Gomer Department of Chemistry James Franck Institute 5640 Ellis Avenue Chicago, Illinois 60637	1
Dr. R. G. Wallis Department of Physics University of California, Irvine Irvine, California 92664	1
Dr. D. Ramaker Chemistry Department George Washington University Washington, D.C. 20052	1
Dr. P. Hansma Physics Department University of California, Santa Barbara Santa Barbara, California 93106	1
Dr. J. C. Hemminger Chemistry Department University of California, Irvine Irvine, California 92717	1
Dr. Martin Fleischmann Department of Chemistry Southampton University Southampton SO9 5NH Hampshire, England	1
Dr. G. Rubloff IBM Thomas J. Watson Research Center P. O. Box 218 Yorktown Heights, New York 10598	1
Dr. J. A. Gardner Department of Physics Oregon State University Corvallis, Oregon 97331	1
Dr. G. D. Stein Mechanical Engineering Department Northwestern University Evanston, Illinois 60201	1
Dr. K. G. Spears Chemistry Department Northwestern University Evanston, Illinois 60201	1
Dr. R. W. Plummer University of Pennsylvania Department of Physics Philadelphia, Pennsylvania 19104	1
Dr. E. Yeager Department of Chemistry Case Western Reserve University Cleveland, Ohio 41106	1
Professor D. Hercules University of Pittsburgh Chemistry Department Pittsburgh, Pennsylvania 15260	1
Professor N. Winograd The Pennsylvania State University Department of Chemistry University Park, Pennsylvania 16802	1
Professor T. F. George The University of Rochester Chemistry Department Rochester, New York 14627	1
Professor Dudley R. Herschbach Harvard College Office for Research Contracts 1350 Massachusetts Avenue Cambridge, Massachusetts 02138	1
Professor Horia Metiu University of California, Santa Barbara Chemistry Department Santa Barbara, California 93106	1
Professor A. Steckl Rensselaer Polytechnic Institute Department of Electrical and Systems Engineering Integrated Circuits Laboratories Troy, New York 12181	1

472:GAN:716-4
94/056

TECHNICAL REPORT DISTRIBUTION LIST, 056

	No. Copies	No. Copies
Dr. John T. Yates Department of Chemistry University of Pittsburgh Pittsburgh, Pennsylvania 15260	1	
Professor G. H. Morrison Department of Chemistry Cornell University Ithaca, New York 14853	1	
Captain Lee Myers AFOSR/NC Bolling AFB Washington, D.C. 20332	1	
Dr. David Squire Army Research Office P. O. Box 12211 Research Triangle Park, NC 27709	1	
Professor Ronald Hoffman Department of Chemistry Cornell University Ithaca, New York 14853	1	


DATE
ILME